A Circularly Polarized Annular-ring Patch Antenna with a Groundplane EBG Annular-slot Array

X.L. Bao, G. Ruvio and M. J. Ammann

Centre for Telecommunications Value-chain Research,
School of Electronic & Communications Engineering,
Dublin Institute of Technology, Kevin Street, Dublin 8, Ireland
Tel: +353 1 402 4716; E-mail: xbao@dit.ie

Abstract—The effects of tuning the parameters of an annular-ring circular patch antenna with a cross-slot are analyzed and discussed. Then, based on this structure, a novel antenna with an electromagnetic bandgap cell system, which consists of a 4×4 annular-slot array in the groundplane, is designed and both numerically and experimentally evaluated. When compared to the annular-ring patch antenna on a groundplane of the same size without EBG structure, the proposed antenna presents a significant increase in the impedance bandwidth, axial-ratio bandwidth and gain. On the other hand, the insertion of the EBG structure allows a 10% reduction of the centre frequency when compared to the annular-ring patch antenna on a conventional groundplane. The simulated and measured results are in good agreement.

Index Terms - Annular-ring patch antenna, Annular-slot, Electromagnetic Bandgap, Circular polarization.

I.INTRODUCTION

Electromagnetic Band Gap (EBG) structures are periodic complex cell systems, which present

bandstop characteristics within a certain frequency range.
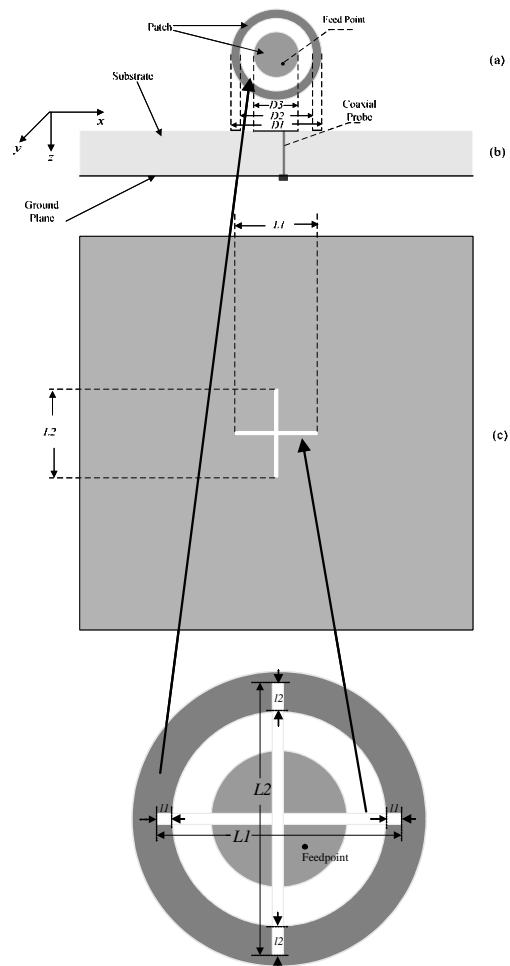
Fig. 1 The geometry of the proposed CP antenna. (a) Top view; (b) Side view; (c) Cross-slot in ground plane

They behave as filters that suppress within a certain frequency range surface waves, which

---

travel on the groundplane and cause diffraction effects. Several EBG techniques have been developed over the last two decades which are applied to microwave circuits and antennas to improve their performance in terms of coupling reduction, low-profile optimization and gain enhancement [1-5]. In addition, they have recently been applied to enhance circularly-polarized (CP) microstrip antenna performance [6, 7].
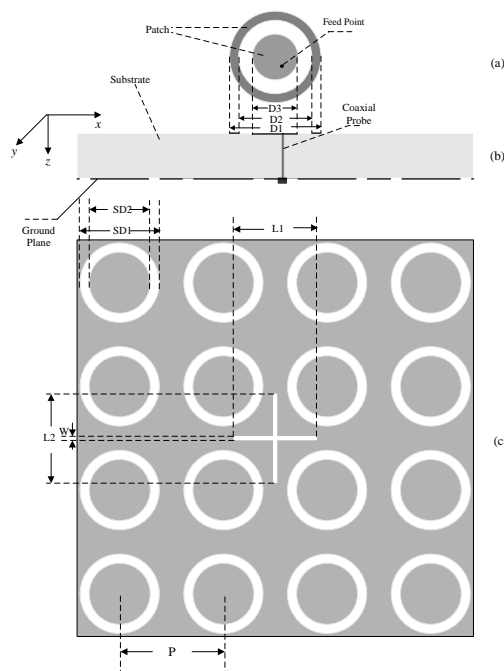
Fig. 2 The geometry of the proposed CP antenna with EBG structure. (a) Top view; (b) Side view; (c) Cross-slot and EBG ground plane.

In this context, annular-ring patch antennas [8, 9] have been very popular due to their compactness compared to other circular and square regular patch antennas with CP properties. In this paper, a circularly polarized annular-ring patch antenna embedded in a particular EBG structure and with an unequal cross-slot in the ground plane is studied and presented. This recently proposed annular-ring antenna structure has been shown to be significantly smaller than conventional annular-ring patch antennas, even on standard groundplanes [10]. By adjusting the length of the two arms of the cross-slot, two orthogonal resonant modes can be obtained and circularly polarized radiation of the proposed antenna will be achieved. A particular EBG structure that

consists of an array of annular slots cut out from the groundplane has been designed to fit into the geometry of the antenna. This structure presents wide stopband characteristics as shown in [11] where the optimum number of EBG cells was determined for this structure. When compared with annular-ring patch antennas without EBG in the same ground plane, the proposed antenna presents an overall better performance. By inserting this EBG structure the input impedance bandwidth increases by over 135% (from 68MHz to 160MHz), the axial-ratio bandwidth over 56% (from 18MHz to 28MHz), and the gain is increased by 3.0dB, compared to the annular-ring patch on conventional groundplane. Simulated and measured results are displayed and discussed below.

II.PARAMETRIC ANALYSIS

Figure 1 shows the geometry of a circular patch antenna loaded by a concentric annular-ring, printed on one side and an unequal cross-slot in the ground plane on the other side. This structure is printed on 1.52mm thick FR4 substrate. This low-cost material presents a permittivity of 4.1 and a loss tanδ of 0.02. The unequal cross-slot can effectively reduce the size of the printed antenna for a given operational frequency. In particular the cross-slot is formed by two orthogonal arms with unequal lateral lengths, *L1* and *L2*, and is coaxial with the circular patch. By adjusting the lengths of the two arms of the cross-slot, the main dip in the input impedance plot can be separated into two near-degenerate resonant modes with equal magnitude and 90 degree phase difference due to the geometry of the slots. When *L2 > L1*, a right hand circular polarization (RHCP) can be obtained, whereas for *L2 < L1* a left hand circular polarization (LHCP) can be achieved. For the proposed CP annular-ring patch antenna on a 130mm×130mm conventional groundplane, the effects of geometric parameters are discussed in detail below.

A. The position of the feedpoint

In order to obtain circular polarization for the proposed antenna, the position of the feedpoint is

located along the 45° diagonal line (as shown on Figure 1).
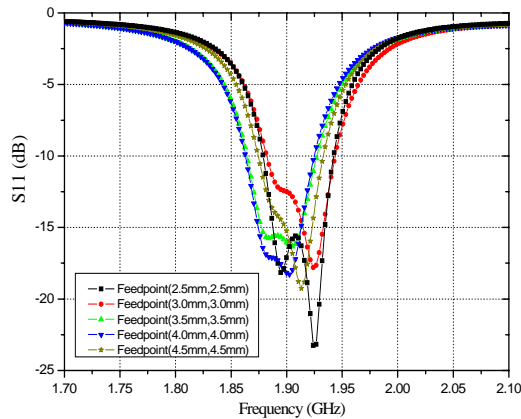
(a)
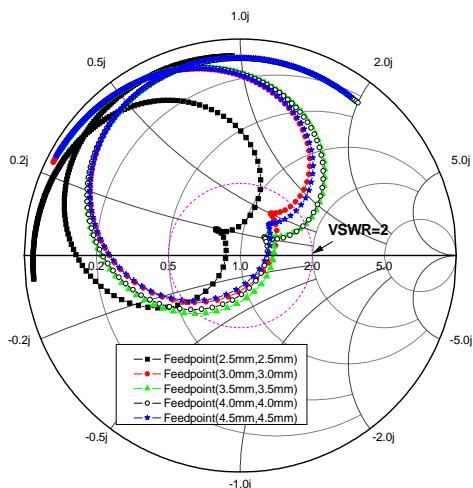
(b)

Fig. 3 The variation in S11 for various feedpoint location. (a) Return loss; (b) Smith chart.

The optimised geometric parameters of the annular-ring antenna are $D1$=30.0mm, $D2$=24.0mm, $D3$=11.0mm, slot width w=1.0mm. The input signal is launched to the radiator by a 50 ohm coaxial probe. In this paper, a RHCP antenna is designed, so that the length of the two arms of the cross-slot are selected to be $L1$=25.0mm, $L2$=27.0mm. The simulated return loss results are displayed in Figure 3a for various positions of feedpoint. From this, it can be seen that as the position of the feedpoint approaches the patch origin, the centre frequency increases and an improvement in matching is observed. The Smith chart is illustrated in Figure 3b. From

the inflection of the different loci, it can be observed that the axial-ratio does not change significantly for the different feed point configurations investigated. So, the feedpoint is selected close to the origin.

B. The length of the cross-slot arms

In order to show the effects of the tuning of the length of the two arms of the cross-slot the other geometric parameter were kept fixed to $D1$=30.0mm, $D2$=24.0mm, $D3$=11.0mm, w=1.0mm and the feedpoint located at (x=2.5mm, y=2.5mm).
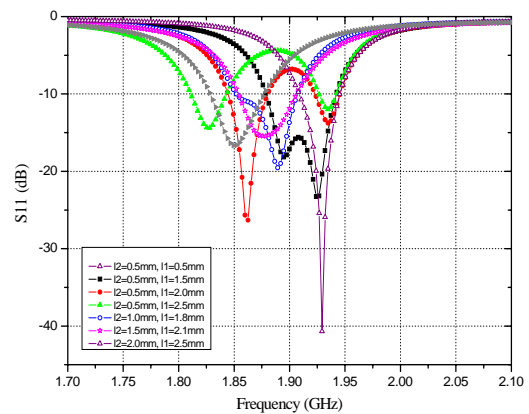
(a)
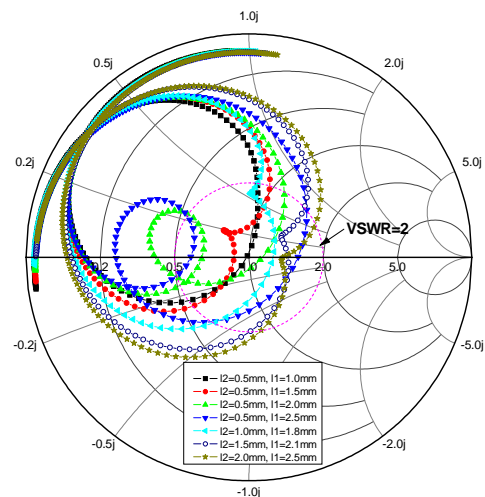
(b)

Fig. 4 The variation in S11 for various lengths of cross-slot. (a) Return loss; (b) Smith chart.

Figure 4a shows the return loss for different combinations of l_1 and l_2. As expected the centre-frequency shifts downwards as the length of the arms increase. At the same time, the impedance matching seems to strongly depend on the slot arms length. Figure 4b shows that when the difference $(l_1 - l_2)$ is about 1mm, we obtain the best performance in terms of both circular polarization and impedance matching.

C. The inner diameter of the annular-ring patch
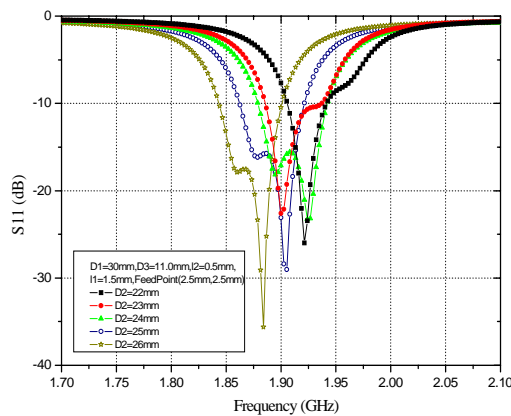
(a)
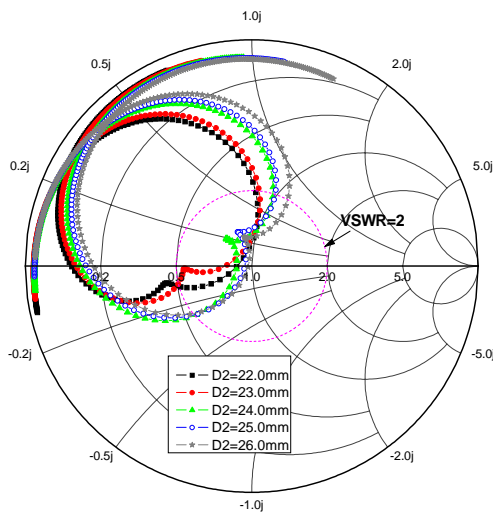
(b)

Fig. 5 The variation in S11 for various diameters *D2* of inner circular patch. (a) Return loss; (b) Smith chart.

For this investigation on tuning the inner diameter of the annular-ring patch the following parameters have been kept constant:

D1=30.0mm, *D3*=11.0mm, *L1*=25.0mm, *L2*=27.0mm, *w*=1.0mm and feedpoint located at (*x*=2.5mm, *y*=2.5mm), whereas the diameter *D2* ranges between 22 and 26mm. The inner diameter of the annular-ring patch appears to be a key parameter as it heavily affects the impedance matching and the resonant frequencies. Figure 5a shows that the propagation of two near-degenerate modes is possible just when *D2* is bigger than 22mm. By observing the same tuning on the Smith chart (Figure 5b), we can find that the point of inflexion that denotes the circularly polarized characteristics shifts towards the matching point, so that we can reduce the resonant frequency and enlarge the width of the axial-ratio bandwidth of the proposed antenna for higher values of *D2*.

D. The diameter of the inner circular patch

Figure 6a and Figure 6b display the return loss and the Smith chart curve of the annular-ring patch antenna for various diameters of the inner circular patch, respectively. We can observe that there is a little effect on the performance of the antenna as the diameter of the inner circular patch increases from 11mm to 18mm. For this investigation, the other geometric parameters were kept constant to the following values: *D1*=30.0mm, *D2*=24.0mm, *L1*=25.0mm, *L2*=27.0mm, *w*=1.0mm, feedpoint located at (2.5mm, 2.5mm).

II. DESIGN OF ANNULAR-RING PATCH ANTENNAS WITH ANNULAR-SLOT ARRAY IN GROUND PLANE

In order to further improve the axial-ratio performance of the proposed antenna, an electromagnetic bandgap structure (EBG) has been designed to match the geometric characteristics of the annular-ring patch (Figure 1B). Numerical results for the proposed antenna have been extracted by the Finite Element Method. The EBG structure is characterised by its period *P*=34.0mm, and the external and internal diameter of the annular slots, *SD1*=26.0mm, *SD2*=20.0mm, respectively. The bandgap of the presented EBG structure has been determined from the *S21* of a transmission
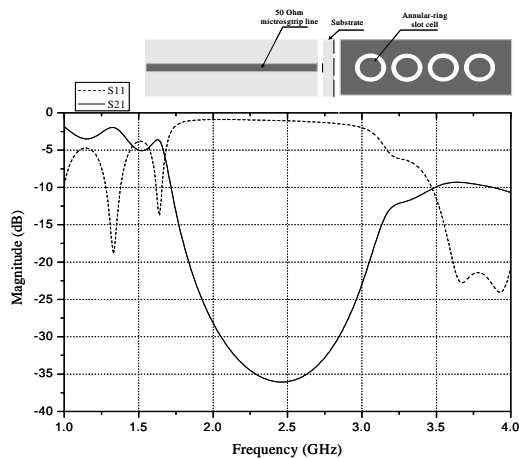
Fig. 7 The simulated S11 and S21 for the annular-ring slot EBG structure.
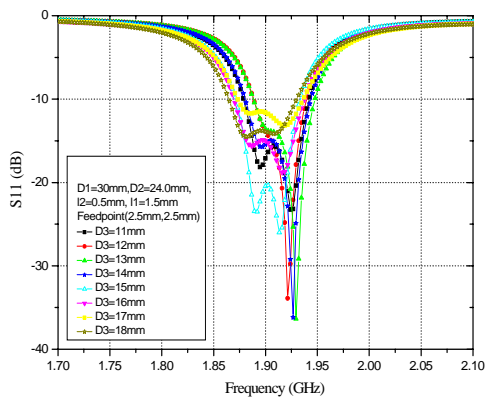
(a)
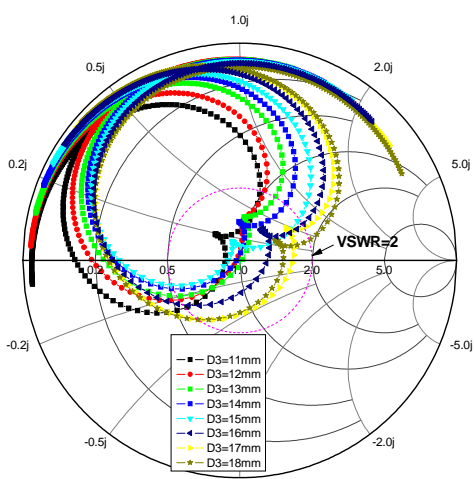
(b)

Fig. 6 The variation in S11 for various inner diameters *D3* of annular-ring patch. (a) Return loss; (b) Smith chart.

line placed on top of a row of 4 cells (Figure 7). Between 1.71GHz and 3.21GHz the transmission coefficient sharply drops below 10dB as a consequence of the resonating behaviour of the EBG cells. In order to compare the effects of this EBG structure on the annular-ring patch antenna, a 4×4 annular-slot array groundplane has been considered. The groundplane size is 130mm×130mm. When the EBG groundplane is inserted, the annular-ring patch antenna must be re-optimized in terms of axial-ratio performance. Figure 8 display the return loss of the antenna optimised with and without EBG cells. In particular, with the EBG groundplane described above, the geometric parameters must be retuned to the following values: *D1*=30.0mm, *D2*=24.0mm, *D3*=15.0mm, *L1*=27.0mm, *L2*=29.0mm, *w*=1.0mm and feedpoint located at (*x*=2.5mm, *y*=2.5mm). From this comparison, it is evident that the proposed annular-ring patch antenna with EBG groundplane presents a notable improvement in terms of impedance bandwidth, and the centre frequency is also reduced by about 10%. A better axial-ratio performance is also achieved with the EBG groundplane as shown on Figure 9.

Antenna1: D1=30mm,D2=24mm,D3=11mm, L1=25mm, L2=27mm
Antenna2: D1=30mm,D2=24mm,D3=15mm, L1=27mm, L2=29mm
- ■ - antenna1
- ▲ - antenna2
- ▼ - antenna1 with EBG
- ● - antenna2 with EBG
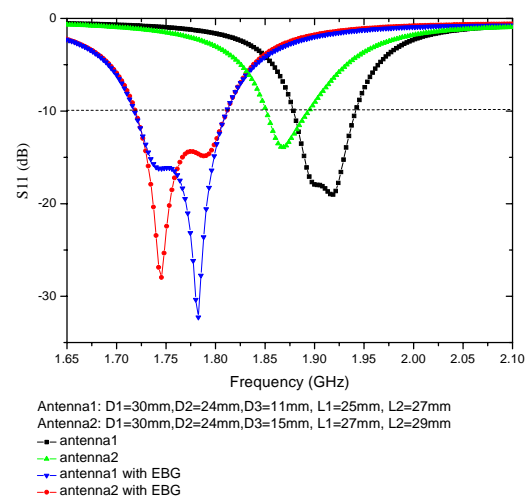
Fig. 8 Simulated comparison of S11of the proposed antenna with and without EBG.
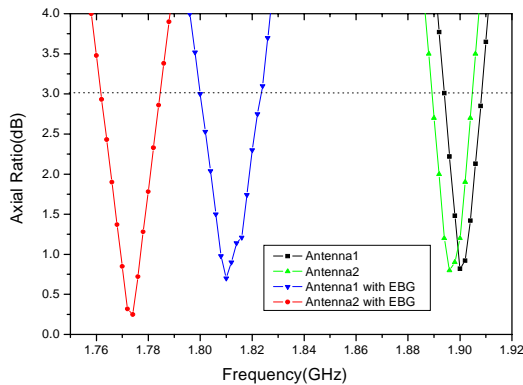
Fig. 9 Simulated comparison of axial-ratio of the proposed antenna with and without EBG.

III.   MEASURED RESULTS

Following the simulated results described above, a prototype of the optimised structure has been realized according the geometric parameters: $D1$=30.0mm, $D2$=24.0mm, $D3$=11.0mm, $L1$=25.0mm, $L2$=27.0mm, w=1.0mm   and feedpoint located at (x=2.5mm, y=2.5mm). The groundplane size is 130mm×130mm and fits a 4×4 array of annular-slots periodically spaced by P=34mm and with external and internal diameter equal   to $SD1$=26.0mm, $SD2$=20.0mm, respectively. Measured and simulated return loss for the same annular-ring patch antennas with and without EBG are presented in Figure 10.

For the antenna on conventional groundplane, the impedance bandwidth is 68MHz, from 1.842GHz to 1.910GHz, but for the EBG antenna, the measured 10dB return loss impedance bandwidth is increased to 160 MHz, from 1.681GHz to 1.841GHz, a significant improvement. The axial-ratio comparison of the antenna with and without EBG is shown in Figure 11. For the antenna without EBG the 3dB axial-ratio bandwidth was found to be 18MHz (1.886GHz to 1.904GHz), but for the EBG antenna, it was 28MHz (1.798GHz to 1.826GHz), an improvement. For the proposed antenna, the spinning dipole radiation pattern at 1.812GHz for the *YoZ* plane is illustrated   in Figure 12a. This pattern shows a wide angular 3dB axial-ratio region across the boresight
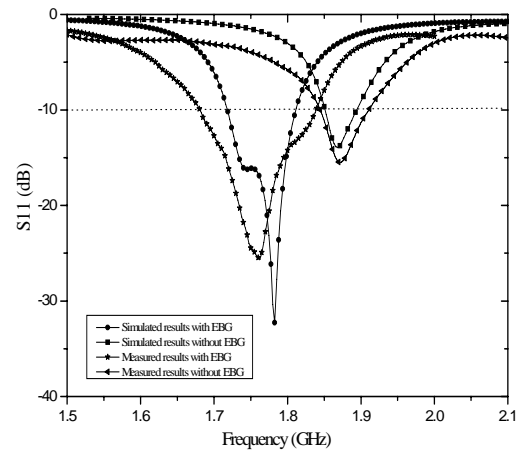
Fig. 10 Measured and simulated S11 of the proposed antenna with and without EBG.
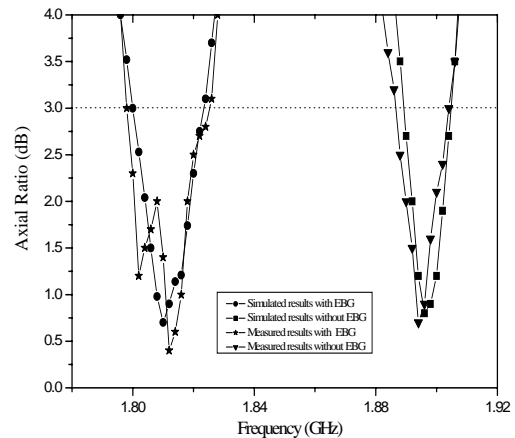
Fig. 11 Measured and simulated axial-ratio of the proposed antenna with and without EBG.

direction and this antenna is reasonably omnidirectional illustrating good CP performance over a broad angular span in the forward half-plane. From Figure 12b, it is noted that cross polarization between the RHCP radiation pattern and the LHCP radiation pattern is at least 25dB. The gain at the centre frequency of 1.812GHz for EBG antenna is 4.2dBi, whereas the gain at the centre frequency of 1.896GHz for the antenna on conventional groundplane is 1.20dBi.

IV.   CONCLUSIONS

A   circularly-polarized   annular-ring   patch antenna with an annular-slot EBG groundplane

is presented, numerically and experimentally. The addition of the EBG groundplane significantly improves the impedance bandwidth, the axial-ratio bandwidth, and the gain performance compared to the same antenna on a conventional groundplane.

(a)

(b)
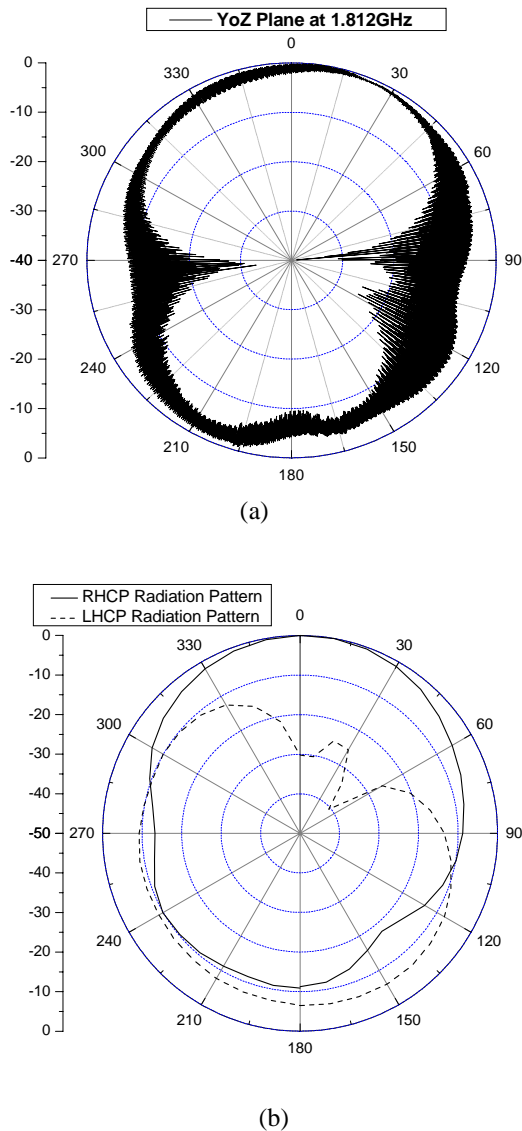
Fig. 12 The measured radiation patterns for the proposed antenna in the *YoZ* plane. (a) The spinning dipole radiation patterns; (b) The co-polarized and cross-polarized radiation pattern at

ACKNOWLEDGEMENT

REFERENCES

[1]. C.Gao, Z.N.Chen, Y.Y.Wang, N.Yang, X.M.Qing, Study and Suppression of Ripples in Passbands of Series/Parallel Loaded EBG Filters, *IEEE Transactions on Microwave Theory and Techniques*, Vol.54, No.4, 2006, pp.1519-1526.

[2]. T.H.Liu,W.X.Zhang, M.Zhang, and K.F.Tsang, Low Profile Spiral Antenna with PBG Substrate, *Electronics Letters*, Vol.36, No.9, 2000, 779-780.

[3]. J.M.Bell, M.F.Iskander, A Low-Profile Archimedean Spiral Antenna Using an EBG Ground Plane, *IEEE Antennas and Wireless Propagation Letters*, Vol.3, 2004, pp.223-226.

[4]. H.Boutayeb, T.A.Denidni, A.R.Sebak, L.Talbi, Design of Elliptical Electromagnetic Bandgap Structures for Directive Antennas, *IEEE Antennas and Wireless Propagation Letters*, Vol.4, 2005, pp.93-96.

[5]. A.Neto, N.Llombart, G.Gerini, P.DeMaagt, On the Optimal Radiation Bandwidth of Printed Slot Antennas Surrounded by EBGs, *IEEE Transactions on Antennas and Propagation*, Vol.54, No.4, April 2006, pp.1074-1083.

[6]. L.I.Basilio, J.T.Williamas, D.R.Jackson and M.A.Khayat, A Comparative Study of a New GPS Reduced-Surface-Wave Antenna, *IEEE Antennas and Wireless Propagation Letters*, 2005, Vol.4, 233-236.

[7]. X.L.Bao, G.Ruvio, M.J.Ammann, and M.John, A Novel GPS Patch Antenna on a Fractal Hi-Impedance Surface Substrate, *IEEE Antennas and Wireless Propagation Letters*, Vol.5, 2006, pp.323-326.

[8]. A.Tavakoli, M.Samiee, G.Z.Rafi, R.Moini, A Time-Domain Analysis of a Wide-Band Circularly-Polarized Crossed-Slot Antenna, *IEEE AP-S International Symposium and URSI Radio Science Meeting*, Baltimore, MD, July 21-26, 1996, pp 2076-2079.

[9]. E.Aloni, and R.Kastner, Analysis of a Dual Circularly Polarized Microstrip Antenna Fed by Crossed Slots, *IEEE Transactions on Antennas and Propagation*, Vol.42, No.8, Aug., 1994, pp.1053-1058.

[10]. X.L.Bao, M.J.Ammann, Compact Annular-ring Embedded Circular Patch Antenna with Cross-slot Ground Plane for Circular Polarisation, *Electronics Letters*, Vo1. 42, No.4, Feb., 2006, pp. 192-193

[11] X.L.Bao, G. Ruvio and M.J.Ammann, Circularly Polarized Annular-ring Patch Antenna with EBG Groundplane, *European Conf. Antennas & Propagation,* 2006, Nice, No. 349921.